Electronic Supplementary Material (ESI) for RSC Advances.


# Stable DNA-based Reaction-Diffusion Patterns

John Zenk[1], Dominic Scalise[1], Kaiyuan Wang[1], Phillip Dorsey[1], Joshua Fern[1], Ariana Cruz[1] and Rebecca Schulman[1,2,*]

[1]Chemical and Biomolecular Engineering and [2]Computer Science, Johns Hopkins University, Baltimore, Maryland 21218, United States

‡Corresponding Author, Rebecca Schulman, Email: rschulm3@jhu.edu

Supporting Information

*Leaks*



***Calibrations***



***1-D Gradients: Experiments and Simulations***



***2-D Gradients: Experiments and Simulations***



***Experimental Setup and Processing***

## Supplementary Note SN1: Leak Reactions and Recapture Kinetics

Leak reactions, or unintended reactions between DNA species which result in Output release or recapture, are a ubiquitous and well documented phenomenon in DNA-based strand displacement systems. Strands and complexes that are less prone to leak can be designed but require more complexity[2]. Previous work [3] documented several types of leak reactions based on molecules similar to those used in this study and are the basis for reactions and leak parameters used in our models here. Such reactions are enumerated in Fig. S10.

Truncated complexes are a possible source of leak reactions. Such complexes can be created when one full length strand and one truncated strand hybridize to form a complex that has a smaller molecular weight than the full-length complex. Such leaky complexes are difficult to distinguish from full-length complexes in a PAGE purification process. Thus, leaky complexes are unintentionally introduced into all experiments. For example, leaky Source complexes occur when the bottom strand of a Source complex is missing bases on its 5' end (Fig. S10(i)), thus providing another reaction mechanism through which a Reporter complex can interact. Further examples of such leaky complexes and their reaction mechanisms can be seen in Fig. S10(ii-iii). Optimizing PAGE protocols to reduce the leak reactions is an ongoing effort, with some changes to protocols described here in Ref. [3].

The quantity of the leaky complexes has been measured in Ref [3], where the authors measured Source strands, similar to those used in this study, with leaky toehold domains to be anywhere between 0.5 and 4.7% of $[S]_0$, and react with rate constant ~50 $M^{-1}s^{-1}$, which is the approximate rate constant for a strand displacement reaction mediated through a two base pair toehold, $k_{2bp}$. For the simulations here we assume that all leak reactions through a truncated strand occur at a reaction rate constant of $k_{2bp} = 50$ $M^{-1}s^{-1}$ and that $[S]_{leak,0} = 0.047[S]_0$, as the bottom strand of the Source species in this paper is longer than in Ref. [3] and therefore we expect the truncation error to be on larger end of the measured range. We also assume that a leaky Recapturer complexes (Fig. S9(iii)) also have an initial concentration of $0.047[Rec]_0$ and react with rate constants of $k_{0bp}$. Although leaky (i.e. unintended), the leak pathway in a recapture reaction is slower and almost insignificant when compared to the primary mechanism of recapture.

While a strand displacement reaction mediated by a nick in a backbone of a DNA duplex, as seen in the Recapturer complex, would typically be expected to produce strand displacement kinetics with forward rates of 0.5 to 5 $M^{-1}s^{-1}$, (which approximately correspond to 0 and 1 bp toehold mediated reaction kinetics, respectively) we found that the Recapture reaction was best modeled with a reaction rate constant of 500 $M^{-1}s^{-1}$ more in line with a 3 bp toehold mediated reaction [1]. Significant fraying of ends can explain the increase in kinetic rates. When analyzed with NUPCK at room temperature, the 1-2 and 3-4 Recapturer complexes have ~50% and ~60% probability, respectively, of having an unpaired base at the nick. To mitigate this fraying in a next generation design, a GC rich region that occludes fraying, for example, can be designed.

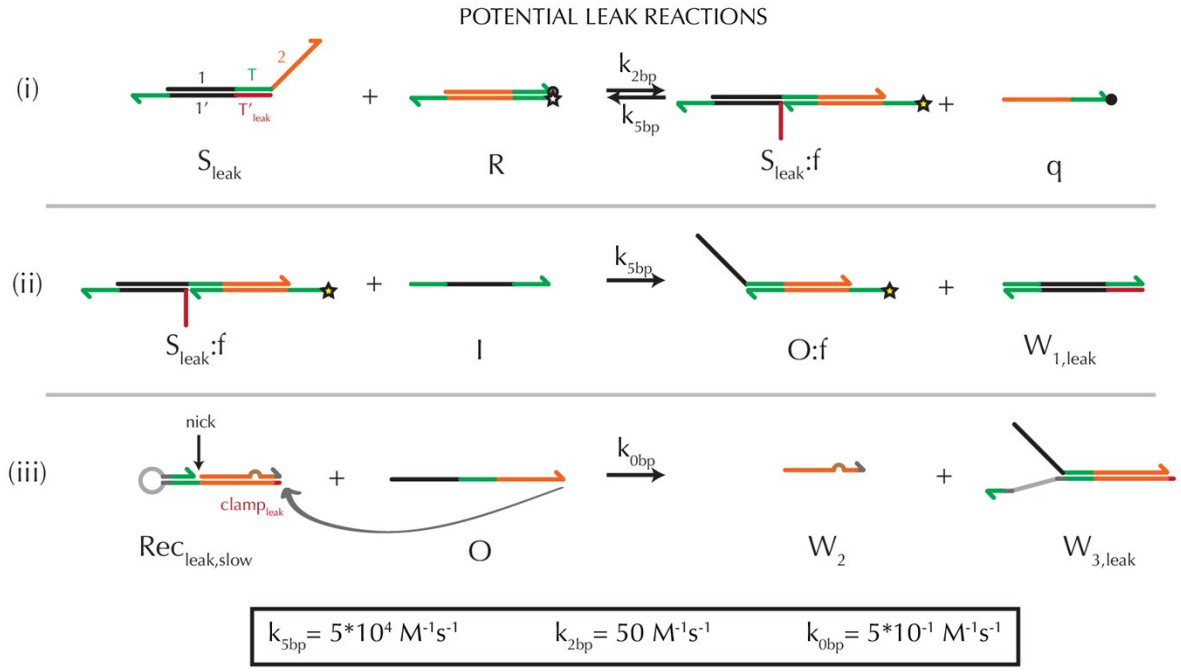


**Figure S1. Potential leak reactions considered in the model.** (i) Reversible reaction between a leaky Source complex ($S_{leak}$) and the Reporter complex, where the leaky Source complex has a bottom strand that is missing some bases (shown in red and labeled $T'_{leak}$). Reaction rate constants shown above and below arrows and their values listed at the bottom of the figure and are estimates from Ref. [1]. We assume a leaky toehold has a -2bp truncation [3] at the 5' end (IDT synthesizes DNA from 3' to 5', thus a truncation error will occur at the 5' end of a strand) and is shown in red. Although we PAGE purify the complexes, we found it challenging to distinguish between complexes with lengths that differ by only a few base pairs in our gels; the primary reason for PAGE purification is to ensure proper stoichiometric ratios of all strands in a complex. Such a source of error could be likely eliminated by purification methods which were able to differentiate between small changes in number of base pairs in a complex, or by ordering purified ssDNA strands. (ii) Irreversible reaction between a leaky Source complex with a fluorophore strand ($S_{leak}$:$f$) and an Initiator through a 5bp toehold-mediated strand displacement reaction to produce an Output:fluorophore and waste complex. (iii) Irreversible reaction between a leaky Recapturer with slow kinetics, where the 5' end of the bottom strand in the Recapturer has two missing bases, therefore the non-reactive clamp would be eliminated, exposing a potential 0bp strand displacement reaction between an Output and the Recapturer. Gray arrow indicates the trajectory of the strand displacement reaction.

**Table ST1: List of reactions modeled in RD system.**

| | | |
|---|---|---|
| **Release** | $S + I \overset{k_{5bp}}{\rightarrow} O + W_1$ | **(1)** |
| **Recapture** | $O + Rec \overset{k_{nick}}{\rightarrow} W_2 + W_3$ | **(2)** |
| **Reporting** | $O + R \underset{k_{5bp}}{\overset{k_{5bp}}{\rightleftharpoons}} f + q$ | **(3)** |
| **LEAK (i)*** | $S_{leak} + R \underset{k_{5bp}}{\overset{k_{2bp}}{\rightleftharpoons}} S_{leak}{:}f + q$ | **(4)** |
| **LEAK (ii)*** | $S_{leak}{:}f + I \overset{k_{5bp}}{\rightarrow} O{:}f + W_{1,leak}$ | **(5)** |
| **Leak (iii)*** | $Rec_{leak,slow} + O \overset{k_{0bp}}{\rightarrow} W_2 + W_{3,leak}$ | **(6)** |

*Leak reactions correspond to those listed in Fig. S10.

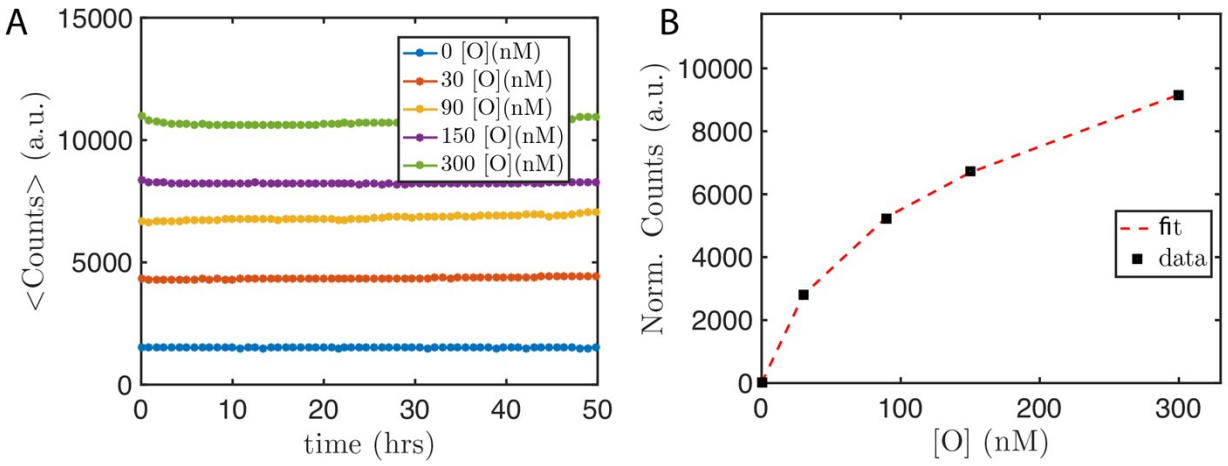


**Figure S2. Calibrating fluorescence.** (A) A typical calibration plot depicting counts from the calibration wells as a function of time. Counts are averaged across entire image. Wells have varying concentration of Output but have a constant amount of Reporter $[R]_0 = 200$ nM in each well. Images are typically taken with an exposure ranging from 50 to 150 ms. (B) The counts are averaged over a period of time, typically 20 hours, and then normalized to zero (such that the average counts at $[O] = 0$ nM are 0). The data is fit to the curve $C_N = \frac{a[O]^2 + b[O] + c}{[O] + d}$ where $a$,$b$,$c$ and $d$ are fitted parameters, $NC$ is the normalized counts and $[O]$ is the Output concentration. This curve is then used to calculate the concentration of the total Output species (unbound Output species + Output species bound to the Reporter), where:

$$[O] = \frac{\sqrt{-4ac + 4adC_N + b^2 - 2bC_N + C_N^2} - b + C_N}{2a}.$$

Where the calibration wells were only fluorescent ssDNA or dsDNA, such as in the diffusion only experiments (see Figure 2 in the main text), the calibration curve was linear and thus fit to a linear equation, $C_N = m[O] + b$ (the fit largely depends on the gain setting used). All calibration wells are comprised of 1% agarose. Calibration wells measured 8x8x8 mm (512 µL).

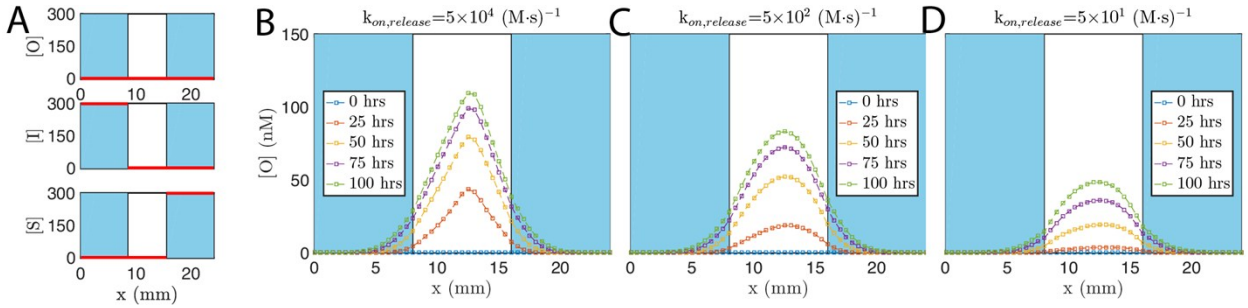


**Figure S3. 1-D Growing Gradient Simulations.** To design a gradient formed by DNA strand displacement processes, we needed to both choose reactions and set the rates for these reactions by choosing the length of the toeholds that initiate the reaction process. To understand how the reaction rate constant for the release reaction would affect the shape of the gradient, we simulated the reaction and diffusion of Source and Initiator species in 1D with measured diffusion coefficients. (A) Initial conditions for the various species in the reservoirs and the agarose gel. The buffer in the liquid reservoirs was exchanged every 24 hours so that these conditions were maintained over time. Blue regions denote liquid reservoirs whereas the white region denotes hydrogel. We simulation the RD using various forward reaction rate constants for the release reaction: (B) $k_{on,release} = 5 \times 10^4$ (M s)$^{-1}$, (B) $5 \times 10^2$ (M s)$^{-1}$ and (C) $50$ (M s)$^{-1}$, which correspond to reactions mediated by approximately 5bp, 3bp, 2bp toeholds respectively[1]. (E) Schematic of the strand displacement process designed to occur at each of the rates considered in simulation. Leak reactions are not included in the simulations shown here.

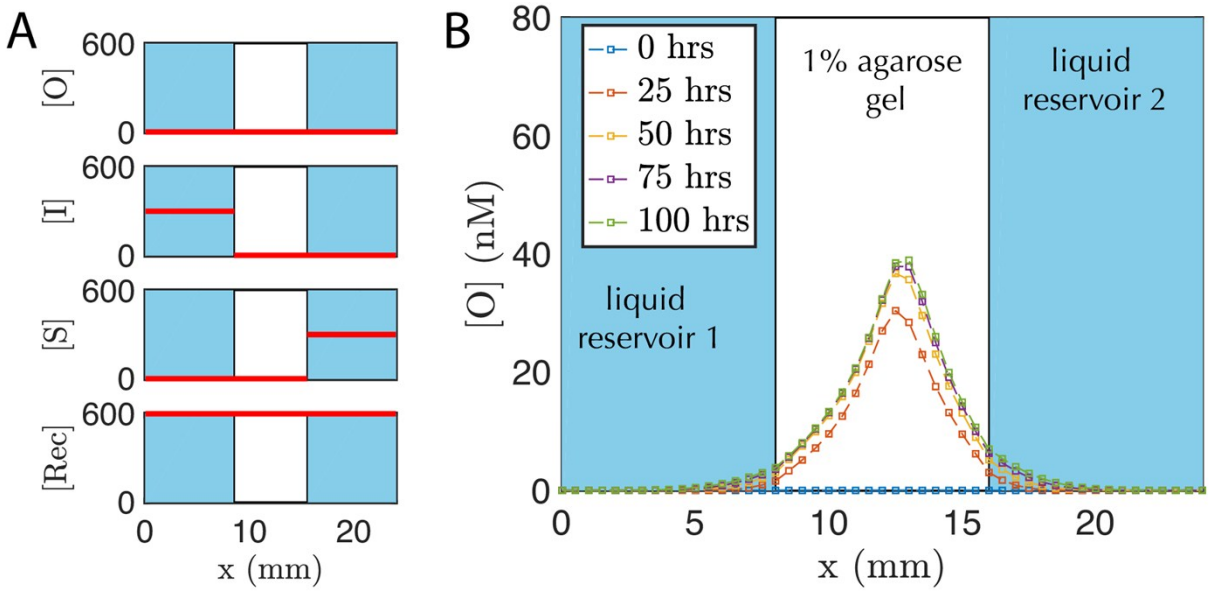


**Figure S4. 1-D Stable Gradient Simulation.** To determine whether 1D gradients formed by release, recapture and reporting reactions in a 1% agarose hydrogel could be stable over time when the liquid reservoirs were periodically refreshed, we simulated the RD system with measured diffusion coefficients and assumed reaction rate constants based on measurements made in solution (see Simulation section in Methods of main text). (A) Initial conditions for the species in the reservoirs and the agarose gel assumed in simulation. Reporter concentration is not shown but is initially 200 nM in both liquid reservoirs and in the hydrogel. (B) Simulations showed that gradients could remain stable once formed. Buffer exchange was simulated in the liquid reservoirs every 24 hours. Blue regions denote liquid reservoirs whereas the white region denotes hydrogel. Leak reactions are not included in the simulations shown here. While the initial conditions of this simulation are identical to those in the experiment shown in Fig. 3C in the main text, the buffer refresh times are slightly different, thus leading to different dynamics.

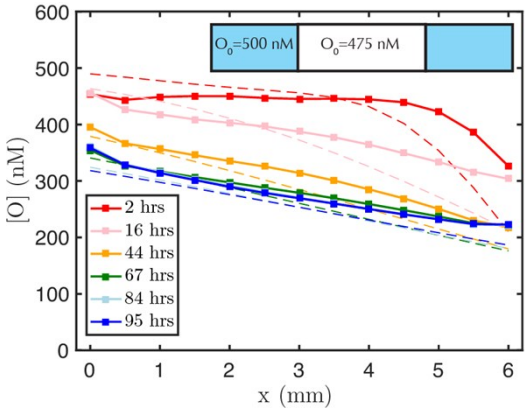


**Figure S5. 1-D Linear Diffusion Gradient.** The inset shows the initial concentrations of the Output in the left reservoir and hydrogel (there is no Output initially in the right reservoir). Solid lines on the plot show the Output concentration as a function of position within the hydrogel and time. Dashed lines are results from a zero parameter-fit simulation, whereas bold lines and squares indicate measured values from experiment (see Methods). The experimentally measured Output concentration at the initial time point were used as initial conditions for the simulation. Initial Reporter concentrations are not depicted for clarity and are $R_0 = 200$ nM in both reservoirs and the hydrogel. The buffers in the reservoirs were exchanged at 24, 51 and 76 hours for fresh buffer containing the initial concentrations of the Output and Reporter.

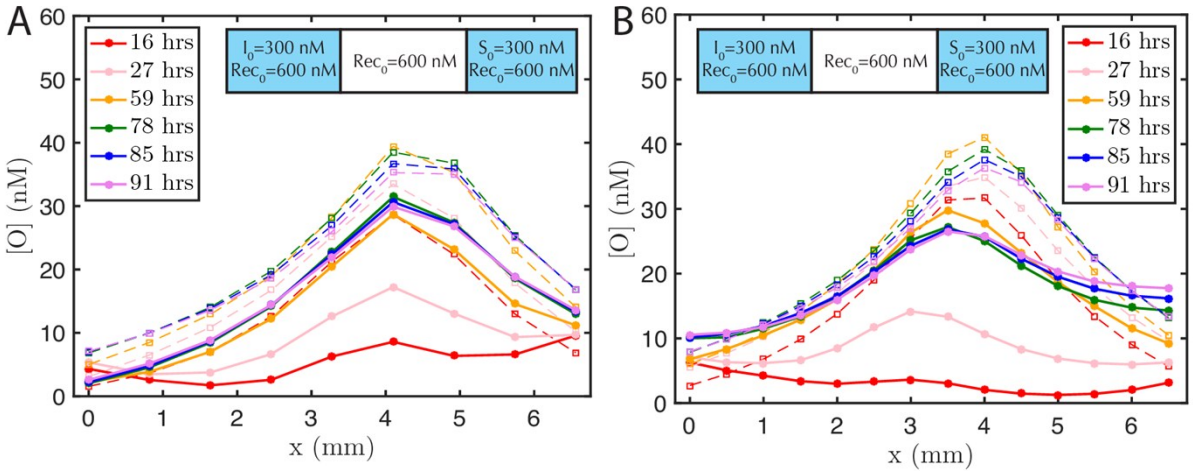


**Figure S6. Stable gradients form consistently.** To characterize the inherent variations expected in the formation of gradient patterns within RD strand displacement systems, we performed two separate experiments in which we formed two stable hill gradients with identical initial and boundary conditions from separate Source, Initiator, Reporter and Recapturer stocks. The two gradients both stabilize in similar periods of time and have similar shapes but differ in peak height and shape. Such differences could be the result in differences in gels, reservoir heights and the purity and effective concentration of the component complexes. Initial conditions of the RD system (the same in both experiments) are depicted in the insets. Initial Reporter concentration is not depicted for clarity and is $R_0 = 200$ nM in the liquid reservoirs and agarose hydrogels for all systems. Inset is a cartoon schematic of the Output species (left) and is the same for both experiments. Buffer exchange occurred after (A) 24 and 52 hours and (B) 48 hours. Differences in simulations between the two figures reflect the different buffer exchange times. (A) 10X objective (IX71 microscope) and (B) 20X objective (IX73 microscope) were used to image the systems.

**2D Gradients: Experiments and Simulations**

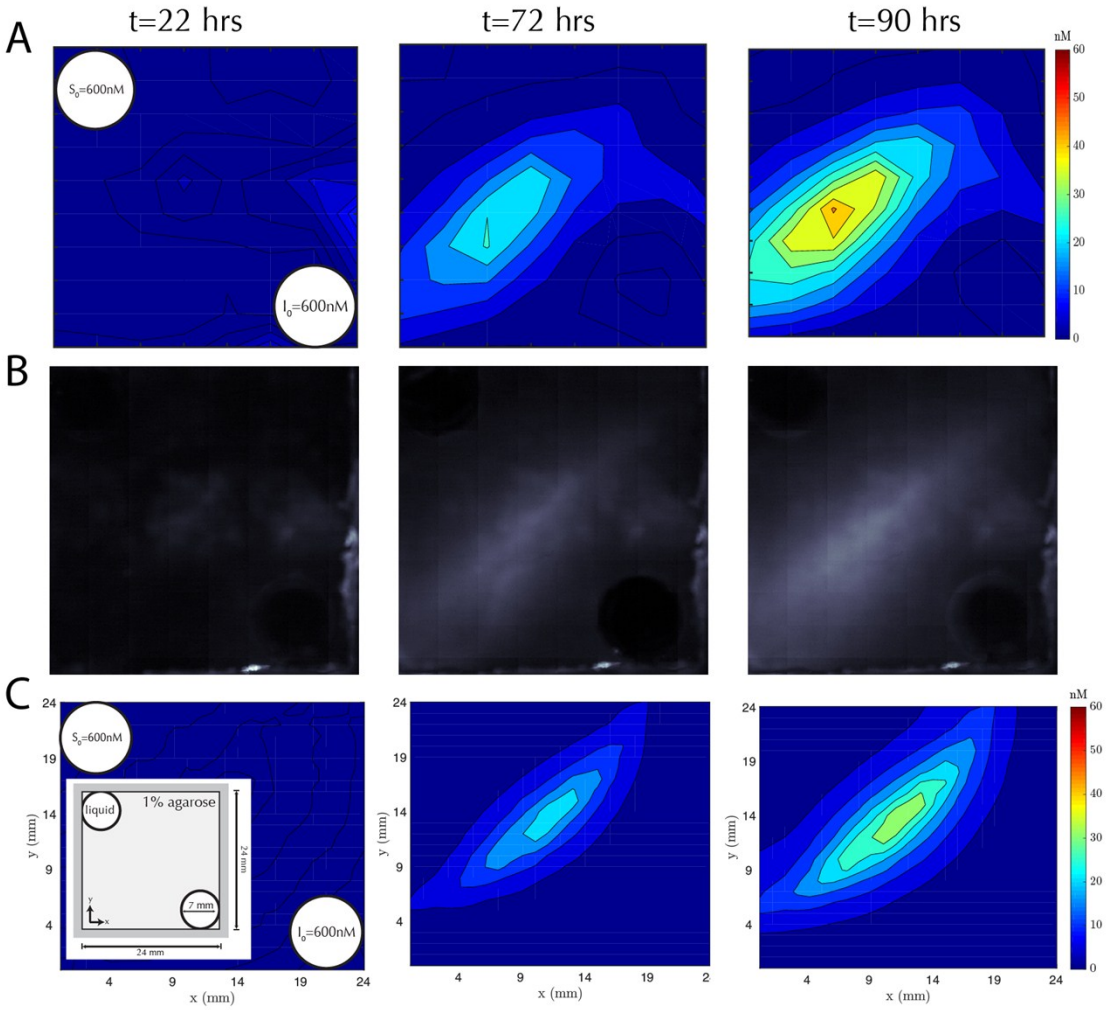


**Figure S7. A large (24 x 24 x 8 mm), growing two-dimensional gradient.** (A) Contour map of the l concentration of Output species in experiment and corresponding (B) optical images used to determine concentrations and (C) simulations at three time points: 22, 72 and 90 hours. The concentrations of source and initiator in the reservoirs at reaction start and after refresh are shown in A and C at 22 hours. Reporter concentration is $R_0 = 200$ nM in both liquid reservoirs and in the agarose gel and is not depicted for clarity. Inset diagram in simulation contour map at 22 hours depicts the schematic for the reaction cell. Fluorescent micrographs are obtained in a raster fashion and stitched together as a mosaic, as the field of view of the 4X objective used is smaller than the RD cell. Dark frame correction was performed for the individual images (see SI Note S2). Buffer was exchanged after 23, 49 and 75 hours.

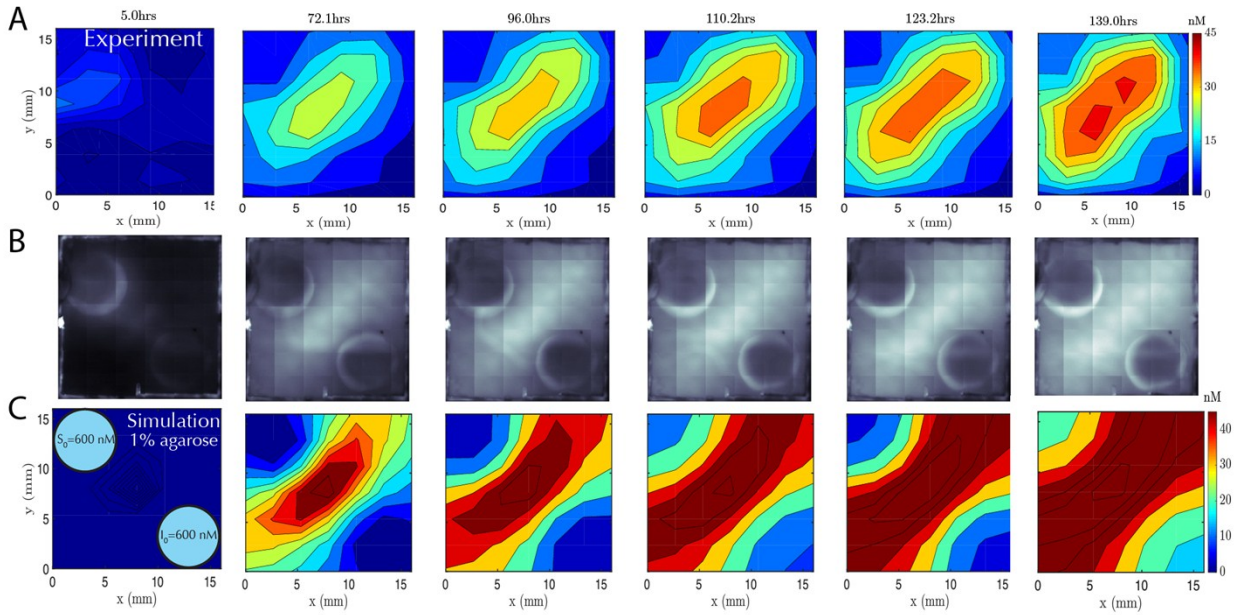


**Figure S8. A medium (16 x 16 x 8 mm), growing two-dimensional gradient.** (A) Filled contour plots depicting the experimental values of Output concentration profile in from 5 hours (left) to 139 hours (right). The gradient continues to grow for at least 139 hours, when the experiment was terminated. Buffer exchange occurred in the experiment after 22, 48, 71, 93 and 116 hours. (B) Corresponding fluorescent micrographs, which are obtained in a raster fashion and stitched together as a mosaic, as the field of view of the 4X objective used is smaller than the RD cell. Dark frame correction was performed for the individual images (see SI Note S2). (C) Filled contour plots depicting the simulated values of Output concentration profile from 5 to 139 hours. Leftmost plot in (C) depicts initial and boundary conditions of species. Reporter concentration is $R_0 = 200$ nM in both liquid reservoirs and in the agarose gel and is not depicted for clarity. See Figure 3 in main text for RD cell cartoon diagram.

## Supplementary Note SN2: Reaction-Diffusion Device Fabrication

To fabricate the PDMS molds we used Sylgard 184 Silicone Elastomer Kit (Dow Corning) and mixed 10:1 of polymer:curing agent. We epoxied 8x8x8 mm wooden cubes (Amazon.com) to the bottom of a weigh boat to create the negative for the mold. Each calibration well was comprised of a single wooden cube and a reaction well was comprised of a linear chain of three cubes so that the 1D RD cell measured 24x8x8 mm (LxWxH) and the calibration wells $(8\ mm)^3$. Two dimensional molds were made from 4 or 9 cubes (dimensions of 16x16x8 or 24x24x8 mm, respectively) and the diameter of the cylindrical wells was 7 mm. The polymer and curing agent were well-mixed, poured into weigh boats and then placed in the desiccator for 90 minutes to eliminate entrapped air bubbles. The device was then cured for 2 hours at 65 °C. The PDMS mold was then extracted from the weigh boat. Dust particles were removed from the PDMS mold using Scotch Tape and the glass slide (48x65 mm, Ted Pella) was cleaned using 70% EtOH and dried with $N_2$. To attach the glass slide to the PDMS, the coverslip and PDMS were treated for ~45 seconds each using a corona surface treater (BD-20, Electro-Technic Products). The device was set at 1.5 hours at 85°C to help promote bonding of the glass to the PDMS.

## Supplementary Note SN3: DNA Sequences

### Diffusion Measurement Experiment

ssDNA used in Diffusion Experiment (shown Figure 2A)
Rb28f: /5TEX615/GTATTGTTGAATTGTAGAGTATT

dsDNA used in Diffusion Experiment (shown Figure 2B)
Rb28f: /5TEX615/GTATTGTTGAATTGTAGAGTATT
Rb28f_full_comp: AATACTCTACAATTCAACAATAC

### 1-2 System

Reversible Reporter 5
Rv5q: CCACCAAACTTCATCTCA/3IABkFQ/
Rb5f: /56-FAM/TGAGATGAAGTTTGGTGGTGAGA

Source 6_5
W6_5: CATAACACAATCACATCTCACCACCAAACTTCA
Gb6(5bp): TGAGATGTGATTGTGTTATGAGATG

Initiator 6
W_6_: CATCTCATAACACAATCACATCTCA

Recapturer 5
Dv5: CACCACCAATCTTCACT
Db5: AGTGAAGTTTGGTGGTGAGATGTTTTTACATCT
(base pair mismatch)

### 3-4 system

Reversible Reporter 28
Rv28q: TCTACAATTCAACAATAC/3IAbRQSp/
Rb28f: /5TEX615/GTATTGTTGAATTGTAGAGTATT

Source 27_28
W27_28: ACAACACTCTATTACAATACTCTACAATTCAAC
Gb6(5bp): TGAGATGTGATTGTGTTATGAGATG

Initiator 27
W_27_: ACAATACAACACTCTATTACAATAC

Recapturer 28
Dv28: ACTCTACAAATCAACAG
Db28: CTGTTGAATTGTAGAGTATTGTATTTTTACAAT
(base pair mismatch)

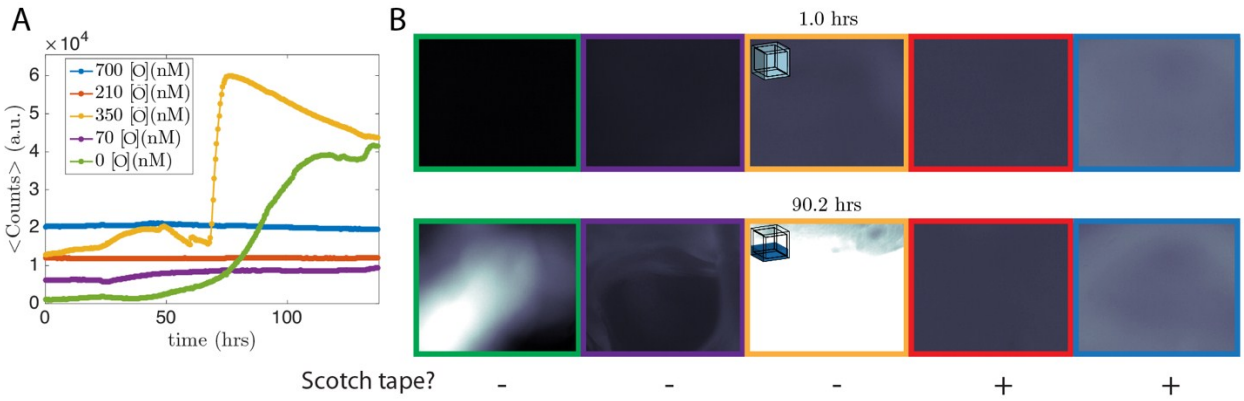


**Figure S9. Preventing Evaporation.** One significant factor in accurately converting fluorescence values to DNA concentrations was ensuring that material did not evaporate during time lapse imaging. Specifically, when covered only with a glass coverslip, almost all of the moisture in the calibration wells would evaporate in ~24-100 hours, leaving the agarose hydrogel at 1-5% of its original volume. This would, in turn increase the fluorescence of the sample as the evaporation process concentrates the DNA species, seen in (A) mean fluorescence vs time of the calibration wells (yellow, green and purple lines) and in the fluorescent images in (B). However, the two calibration wells sealed with Scotch tape did not significantly change fluorescence over the course of 130 hours (red and blue lines). Thus, we sealed all calibration and reaction channels with Scotch tape to mitigate evaporation. Border color in optical images (right side) corresponds with line color in plot. Optical images are shown after 1 hour (above) and 90.2 hours (below). Inset cartoon cube diagrams show (above) a calibration well full of agarose solution with DNA and (below) a well after some evaporation resulting in a solution that is more concentrated in DNA species.

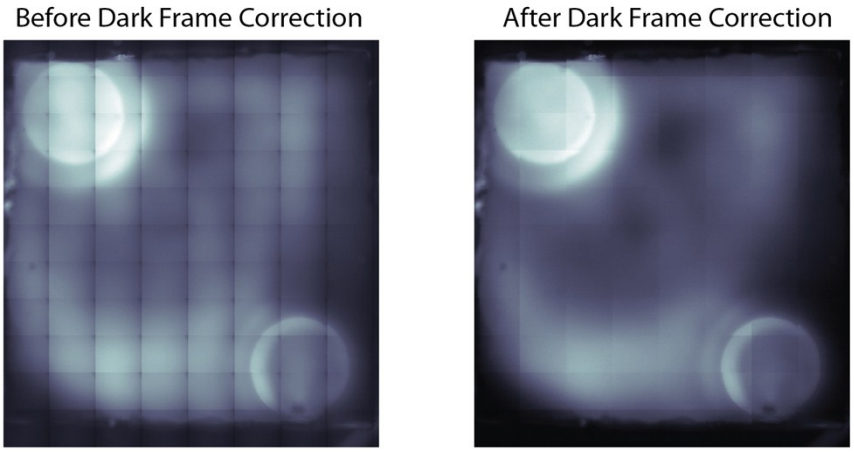


**Figure S10. Dark frame correction to reduce edge effects in image montages.** For the sake of continuity in fluorescence images, we eliminated the majority of the edge effects (typically a darker ring around the outer pixels) by using standard dark frame correction algorithms. While still not perfect, the dark frame correction eliminates the majority of the imaging artifacts. A more sophisticated algorithm like flat fielding would likely eliminate more edge effects, however, it seemed infeasible to obtain the necessary uniformly-lit images for every image in the set. Immediately after image acquisition, we use a binning algorithm to compress the images, as a typical experiment captures ~20,000 images and an image captured on the 16-bit Infinity 3 CCD camera has 2752 x 2192 pixels (which would amount to ~240 Gb of data per experiment). The binning algorithm takes the mean intensity value of the nearest 4x4 pixels and stores the resulting value as a new pixel (resulting in a 16X compression).

## Supplementary References


1. D. Y. Zhang and E. Winfree, *J Am Chem Soc*, 2009, **131**, 17303-17314.
2. C. Thachuk, E. Winfree and D. Soloveichik, in *DNA Computing and Molecular Programming: 21st International Conference, DNA 21, Boston and Cambridge, MA, USA, August 17-21, 2015. Proceedings*, eds. A. Phillips and P. Yin, Springer International Publishing, Cham, 2015, DOI: 10.1007/978-3-319-21999-8_9, pp. 133-153.
3. J. Fern, D. Scalise, A. Cangialosi, D. Howie, L. Potters and R. Schulman, *ACS Synthetic Biology*, 2016, DOI: 10.1021/acssynbio.6b00170.